# A Learning-Based Approach for Traffic State Reconstruction from Limited Data

Nail Baloul, Amaury Hayat, Thibault Liard, Pierre Lissy

SMAI 2025, Carcans Maubuisson

June, 3rd 2025

# Outline

## Table of Contents

# Motivation

Traffic jam in Beijing

- Traffic congestion is a main contributor of air pollution and excessive travel time
  $\Rightarrow$ impacts urban mobility and environmental quality

# Motivation

Traffic jam in Beijing

- Traffic congestion is a main contributor of air pollution and excessive travel time
  $\Rightarrow$ impacts urban mobility and environmental quality
- Traffic management relies on **control** schemes to address perturbed traffic conditions
- Most existing control techniques require complete and accurate knowledge of state
- In practice, full information is rarely available due to limited and noisy measurements

# Motivation

Traffic jam in Beijing

- Traffic congestion is a main contributor of air pollution and excessive travel time
  $\Rightarrow$ impacts urban mobility and environmental quality
- Traffic management relies on **control** schemes to address perturbed traffic conditions
- Most existing control techniques require complete and accurate knowledge of state
- In practice, full information is rarely available due to limited and noisy measurements
- **Goal** $\Rightarrow$ develop reliable methods for **estimating traffic from partial data**

# Traffic Flow Modeling Scales

Benchmark scales of traffic models

- microscopic $\Rightarrow$ individual vehicle dynamics, full information given

## Microscopic model

- Simulation of agent-based dynamics
- Tracking position $x_i(t)$, velocity $v_i(t)$ of vehicle $i$ at time $t$
- Each driver responds to surrounding traffic by adjusting his speed

$$\dot{v}_i(t) = F(v_i(t), x_i(t)) \qquad (1)$$

# Traffic Flow Modeling Scales

Benchmark scales of traffic models

- macroscopic $\Rightarrow$ continuum representation using aggregated variables

## Macroscopic model

- Traffic modelled as a continuous flow
- Density $\rho(t,x)$, speed $v(\rho)$, flux $f(\rho)$
- Total number of cars is conserved

$$
\begin{aligned}
0 &= \frac{d}{dt}\int_a^b \rho(t,x)dx \\
&= f(\rho(t,a)) - f(\rho(t,b)) \qquad (2) \\
&= -\int_a^b \frac{\partial}{\partial x} f(\rho(t,x))dx
\end{aligned}
$$

# Traffic Flow Modeling Scales

Benchmark scales of traffic models

- microscopic $\Rightarrow$ individual vehicle dynamics, full information given
- macroscopic $\Rightarrow$ continuum representation using aggregated variables

## Microscopic model

- Simulation of agent-based dynamics
- Tracking position $x_i(t)$, velocity $v_i(t)$ of vehicle $i$ at time $t$
- Each driver responds to surrounding traffic by adjusting his speed

$$\dot{v}_i(t) = F(v_i(t), x_i(t)) \tag{1}$$

## Macroscopic model

- Traffic modelled as a continuous flow
- Density $\rho(t,x)$, speed $v(\rho)$, flux $f(\rho)$
- Total number of cars is conserved

$$\begin{aligned} 0 =& \frac{d}{dt}\int_a^b \rho(t,x)dx \\ =& f(\rho(t,a)) - f(\rho(t,b)) \\ =& -\int_a^b \frac{\partial}{\partial x} f(\rho(t,x))dx \end{aligned} \tag{2}$$

- **Connection** $\Rightarrow$ macroscopic variables emerge from microscopic interactions

# Table of Contents

- Follow-the-Leader (FtL), **microscopic** first order model
  $\Rightarrow$ dynamics of each vehicle depend on vehicle immediately in front

$$\begin{cases} \dot{x}_N^N(t) = v_{\max}, & t > 0, \\ \dot{x}_i^N(t) = v\left(\frac{L}{N(x_{i+1}^N(t) - x_i^N(t))}\right), & t > 0, \quad i = 0, \cdots, N-1 \\ x_i^N(0) = \bar{x}_i^N, & i = 0, \cdots, N \end{cases} \tag{3}$$

$\Rightarrow$ accurate traffic representation, encodes individual movements
$\Rightarrow$ computationally demanding, requires more data

# Model-Based Approaches

- Follow-the-Leader (FtL), **microscopic** first order model
  $\Rightarrow$ dynamics of each vehicle depend on vehicle immediately in front

$$\begin{cases} \dot{x}_N^N(t) = v_{\max}, & t > 0, \\ \dot{x}_i^N(t) = v\left(\frac{L}{N(x_{i+1}^N(t) - x_i^N(t))}\right), & t > 0, \quad i = 0, \cdots, N-1 \\ x_i^N(0) = \bar{x}_i^N, & i = 0, \cdots, N \end{cases} \tag{3}$$

  $\Rightarrow$ accurate traffic representation, encodes individual movements
  $\Rightarrow$ computationally demanding, requires more data

- Lighthill-William-Richards (LWR), **macroscopic** traffic flow model
  $\Rightarrow$ vehicles treated as a continuous medium similar to particles in fluid
  $\Rightarrow$ one-dimensional (hyperbolic) conservation law

$$\begin{cases} \frac{\partial}{\partial t}\rho(t,x) + \frac{\partial}{\partial x} f(\rho(t,x)) = 0, & x \in \mathbb{R}, \quad t > 0, \\ \rho(x,0) = \rho_0(x), & x \in \mathbb{R} \end{cases} \tag{4}$$

  $\Rightarrow$ faster implementation, less data-intensive
  $\Rightarrow$ overlooks traffic heterogeneity, oversimplifies traffic phenomena

- **Convergence analysis of FtL approximation scheme towards LWR model**[1]

[1] Holden and Risebro 2017.

[2] Di Francesco and Rosini 2015.

- **Convergence analysis of FtL approximation scheme towards LWR model**[1]
- Link between FtL and LWR based on atomization of initial density $\rho_0$

$$\bar{x}_{i+1}^N := \sup\left\{x \in \mathbb{R} : \int_{\bar{x}_i^N}^{x} \rho_0(y)dy = \frac{L}{N}\right\}, \quad i = 0, \cdots, N-1 \tag{5}$$

[1] Holden and Risebro 2017.

[2] Di Francesco and Rosini 2015.

- **Convergence analysis of FtL approximation scheme towards LWR model**[1]
- Link between FtL and LWR based on atomization of initial density $\rho_0$

$$\bar{x}_{i+1}^N := \sup\left\{x \in \mathbb{R} : \int_{\bar{x}_i^N}^{x} \rho_0(y)dy = \frac{L}{N}\right\}, \quad i = 0, \cdots, N-1 \tag{5}$$

- Solution of PDE (3) can be recovered as many particle limit[2] of ODE system (4)

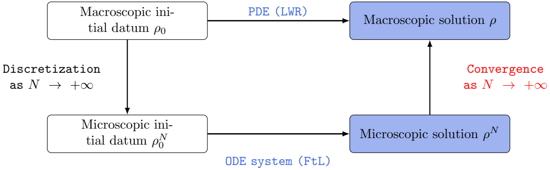


Coupled Resolution of a Microscopic ODE System and a Macroscopic PDE

[1] Holden and Risebro 2017.

[2] Di Francesco and Rosini 2015.

- Hybrid micro-macro models explored in traffic density reconstruction[3]

$$\begin{cases} \dot{x}_N^N(t) = v_{\max}, & t > 0, \\ \dot{x}_i^N(t) = v\left(\rho(t, x_i^N(t))\right), & t > 0,, \quad i = 0, \cdots, N-1 \\ \frac{\partial}{\partial t}\rho(t,x) + \frac{\partial}{\partial x} f(\rho(t,x)) = \gamma^2 \frac{\partial^2}{\partial x^2}\rho(t,x), & x \in \mathbb{R}, \quad t > 0, \end{cases} \tag{6}$$

[3]Barreau, Aguiar, Liu, and Johansson 2021.
[4]Liu, Barreau, Cicic, and Johansson 2020.

- Hybrid micro-macro models explored in traffic density reconstruction[3]

$$\begin{cases} \dot{x}_N^N(t) = v_{\max}, & t > 0, \\ \dot{x}_i^N(t) = v\left(\rho(t, x_i^N(t))\right), & t > 0,, \quad i = 0, \cdots, N-1 \\ \frac{\partial}{\partial t}\rho(t,x) + \frac{\partial}{\partial x} f(\rho(t,x)) = \gamma^2 \frac{\partial^2}{\partial x^2}\rho(t,x), & x \in \mathbb{R}, \quad t > 0, \end{cases} \tag{6}$$

- **Partial state reconstruction**[4] using measurements from probe vehicles (PVs)
  $\Rightarrow$ low penetration rate $N_{\text{probes}} \ll N_{\text{total}}$
  $\Rightarrow$ recover density $\rho$ from **limited** trajectories

[3]Barreau, Aguiar, Liu, and Johansson 2021.
[4]Liu, Barreau, Cicic, and Johansson 2020.

- Hybrid micro-macro models explored in traffic density reconstruction[3]

$$\begin{cases} \dot{x}_N^N(t) = v_{\max}, & t > 0, \\ \dot{x}_i^N(t) = v\left(\rho(t, x_i^N(t))\right), & t > 0,, \quad i = 0, \cdots, N-1 \\ \frac{\partial}{\partial t}\rho(t,x) + \frac{\partial}{\partial x} f(\rho(t,x)) = \gamma^2 \frac{\partial^2}{\partial x^2}\rho(t,x), & x \in \mathbb{R}, \quad t > 0, \end{cases} \tag{6}$$

- **Partial state reconstruction**[4] using measurements from probe vehicles (PVs)
  $\Rightarrow$ low penetration rate $N_{\text{probes}} \ll N_{\text{total}}$
  $\Rightarrow$ recover density $\rho$ from **limited** trajectories
- Requires access to real-time positions, densities and instantaneous speeds of PVs

[3] Barreau, Aguiar, Liu, and Johansson 2021.
[4] Liu, Barreau, Cicic, and Johansson 2020.

- Hybrid micro-macro models explored in traffic density reconstruction[3]

$$\begin{cases} \dot{x}_N^N(t) = v_{\max}, & t > 0, \\ \dot{x}_i^N(t) = v\left(\rho(t, x_i^N(t))\right), & t > 0,, \quad i = 0, \cdots, N-1 \\ \frac{\partial}{\partial t}\rho(t,x) + \frac{\partial}{\partial x} f(\rho(t,x)) = \gamma^2 \frac{\partial^2}{\partial x^2}\rho(t,x), & x \in \mathbb{R}, \quad t > 0, \end{cases} \tag{6}$$

- **Partial state reconstruction**[4] using measurements from probe vehicles (PVs)
  $\Rightarrow$ low penetration rate $N_{\text{probes}} \ll N_{\text{total}}$
  $\Rightarrow$ recover density $\rho$ from **limited** trajectories
- Requires access to real-time positions, densities and instantaneous speeds of PVs
- Prior approaches rely on knowledge of initial density $\rho_0$
  $\Rightarrow$ **No access** to this critical information, need to leverage available data

[3] Barreau, Aguiar, Liu, and Johansson 2021.
[4] Liu, Barreau, Cicic, and Johansson 2020.

# Table of Contents

# Parametrized Microscopic Model

- **Limited data scenario** $\Rightarrow$ only **initial and final** $\left\{\left(\bar{x}^N, \bar{y}^N\right)\right\}_{i=0}^{n}$ positions of PVs

# Parametrized Microscopic Model

- **Limited data scenario** $\Rightarrow$ only **initial and final** $\left\{\left(\bar{x}^N, \bar{y}^N\right)\right\}_{i=0}^{n}$ positions of PVs
- **Enhanced** version of FtL scheme (3) adding a parameter
  $\Rightarrow$ $\alpha^N$ accounts for unobserved vehicles between consecutive PVs
  $\Rightarrow$ adjusts dynamics and allows varying levels of response
  $\Rightarrow$ bridges discrete (vehicle-level) dynamics to continuous (density-level) dynamics

# Parametrized Microscopic Model

- **Limited data scenario** $\Rightarrow$ only **initial and final** $\left\{\left(\bar{x}^N, \bar{y}^N\right)\right\}_{i=0}^{n}$ positions of PVs
- **Enhanced** version of FtL scheme (3) adding a parameter
  $\Rightarrow$ $\alpha^N$ accounts for unobserved vehicles between consecutive PVs
  $\Rightarrow$ adjusts dynamics and allows varying levels of response
  $\Rightarrow$ bridges discrete (vehicle-level) dynamics to continuous (density-level) dynamics
- Parametrized ODE system with finite time horizon

$$\begin{cases} \dot{x}_n^N(t) = v_{\max}, & t \in (0, T] \\ \dot{x}_i^N(t) = v\left(\rho_i^N(t)\right), & t \in (0, T] \quad i = 0, \cdots, n-1 \\ x_i^N(0) = \bar{x}_i^N, & i = 0, \cdots, n \end{cases} \tag{7}$$

$\Rightarrow$ local discrete densities

$$\rho_i^N(t) := \frac{\alpha_i^N L}{N\left(x_{i+1}^N(t) - x_i^N(t)\right)}, \quad t \in (0, T], \quad i = 0, \cdots, n-1 \tag{8}$$

- **Limited data scenario** $\Rightarrow$ only **initial and final** $\left\{\left(\bar{x}^N, \bar{y}^N\right)\right\}_{i=0}^{n}$ positions of PVs
- **Enhanced** version of FtL scheme (3) adding a parameter
  $\Rightarrow$ $\alpha^N$ accounts for unobserved vehicles between consecutive PVs
  $\Rightarrow$ adjusts dynamics and allows varying levels of response
  $\Rightarrow$ bridges discrete (vehicle-level) dynamics to continuous (density-level) dynamics
- Parametrized ODE system with finite time horizon

$$\begin{cases} \dot{x}_n^N(t) = v_{\max}, & t \in (0, T] \\ \dot{x}_i^N(t) = v\left(\rho_i^N(t)\right), & t \in (0, T] \quad i = 0, \cdots, n-1 \\ x_i^N(0) = \bar{x}_i^N, & i = 0, \cdots, n \end{cases} \tag{7}$$

$\Rightarrow$ local discrete densities

$$\rho_i^N(t) := \frac{\alpha_i^N L}{N\left(x_{i+1}^N(t) - x_i^N(t)\right)}, \quad t \in (0, T], \quad i = 0, \cdots, n-1 \tag{8}$$

- Piecewise constant Eulerian discrete density

$$\rho^N(t,x) := \sum_{i=0}^{N-1} \rho_i^N(t) \chi_{[x_i^N(t), x_{i+1}^N(t))}(x), \quad x \in \mathbb{R}, \quad t \in [0, T] \tag{9}$$

# Well Posedness

- Assumptions on velocity

$$v \in C^1([0, +\infty)) \tag{10a}$$

$$v \text{ is decreasing on } [0, +\infty) \tag{10b}$$

$$v(0) = v_{\max} < \infty \tag{10c}$$

[5] Di Francesco, Fagioli, Rosini, and Russo 2016.

# Well Posedness

- Assumptions on velocity

$$v \in C^1([0, +\infty)) \tag{10a}$$
$$v \text{ is decreasing on } [0, +\infty) \tag{10b}$$
$$v(0) = v_{\max} < \infty \tag{10c}$$

- Local existence and uniqueness of solution to (7) (for fixed $\alpha$) via Picard-Lindelöf

[5] Di Francesco, Fagioli, Rosini, and Russo 2016.

- Assumptions on velocity

$$v \in C^1([0,+\infty)) \tag{10a}$$
$$v \text{ is decreasing on } [0,+\infty) \tag{10b}$$
$$v(0) = v_{\max} < \infty \tag{10c}$$

- Local existence and uniqueness of solution to (7) (for fixed $\alpha$) via Picard-Lindelöf
- Condition on initial car positions $\bar{x}_0^N < \bar{x}_1^N < \cdots < \bar{x}_{n-1}^N < \bar{x}_n^N$
  $\Rightarrow$ global existence

**Lemma (Discrete maximum principle)**

*For solution $x(t)$ of (7) with $v$ satisfying (10a)-(10c), for all $i = 0, \cdots, n-1$,*

$$\frac{\alpha_i^N L}{NM} \le x_{i+1}^N(t) - x_i^N(t) \le \bar{x}_n^N - \bar{x}_0^N + (v_{\max} - v(M))\, t, \quad \forall t \in [0, T], \tag{11}$$

*where* $M := \max_i \left( \frac{\alpha_i^N L}{N(\bar{x}_{i+1}^N - \bar{x}_i^N)} \right)$

[5] Di Francesco, Fagioli, Rosini, and Russo 2016.

- Assumptions on velocity

$$v \in C^1([0,+\infty)) \tag{10a}$$
$$v \text{ is decreasing on } [0,+\infty) \tag{10b}$$
$$v(0) = v_{\max} < \infty \tag{10c}$$

- Local existence and uniqueness of solution to (7) (for fixed $\alpha$) via Picard-Lindelöf
- Condition on initial car positions $\bar{x}_0^N < \bar{x}_1^N < \cdots < \bar{x}_{n-1}^N < \bar{x}_n^N$
  $\Rightarrow$ global existence

**Lemma (Discrete maximum principle)**

*For solution $x(t)$ of (7) with $v$ satisfying (10a)-(10c), for all $i = 0, \cdots, n-1$,*

$$\frac{\alpha_i^N L}{NM} \leq x_{i+1}^N(t) - x_i^N(t) \leq \bar{x}_n^N - \bar{x}_0^N + (v_{\max} - v(M))\, t, \quad \forall t \in [0, T], \tag{11}$$

*where* $M := \max_i \left( \frac{\alpha_i^N L}{N(\bar{x}_{i+1}^N - \bar{x}_i^N)} \right)$

- $\rho^N$ discrete approximation[5] of solution to LWR model (4)

[5] Di Francesco, Fagioli, Rosini, and Russo 2016.

# ODE-Contrained Optimization

- Physical conditions on $\alpha := \alpha^N$ induce feasible set

$$\mathcal{A}_N := \left\{ \alpha \in \mathbb{R}^n : \quad \alpha_i \in \left[1, \bar{z}_i^N\right], \quad i = 0, \dots, n-1, \quad \sum_{i=0}^{n-1} \alpha_i = N \right\} \tag{12}$$

with $\bar{z}_i^N := \min \left\{ \frac{N\left(\bar{x}_{i+1}^N - \bar{x}_i^N\right)}{L}, \frac{N\left(\bar{y}_{i+1}^N - \bar{y}_i^N\right)}{L} \right\}, \quad i = 0, \dots, n-1$

[6] Baloul, Hayat, Liard, and Lissy 2025.

- Physical conditions on $\alpha := \alpha^N$ induce feasible set

$$\mathcal{A}_N := \left\{ \alpha \in \mathbb{R}^n : \quad \alpha_i \in \left[1, \bar{z}_i^N\right], \quad i = 0, \ldots, n-1, \quad \sum_{i=0}^{n-1} \alpha_i = N \right\} \tag{12}$$

with $\bar{z}_i^N := \min \left\{ \frac{N\left(\bar{x}_{i+1}^N - \bar{x}_i^N\right)}{L}, \frac{N\left(\bar{y}_{i+1}^N - \bar{y}_i^N\right)}{L} \right\}, \quad i = 0, \ldots, n-1$

- **Approximate density reconstruction**[6] $\Rightarrow$ find optimal interaction parameter $\alpha$

$$\begin{aligned} & \underset{\alpha}{\text{minimize}} \quad \frac{1}{2} \left\| x(T) - \bar{y} \right\|^2 \\ \text{s.t.} \quad & \dot{x}(t) = V\left(W_\alpha x(t) + b_\alpha(t)\right) \\ & x(0) = \bar{x} \\ & \alpha \in \mathcal{A}_N \end{aligned} \tag{13}$$

[6] Baloul, Hayat, Liard, and Lissy 2025.

- Physical conditions on $\alpha := \alpha^N$ induce feasible set

$$\mathcal{A}_N := \left\{ \alpha \in \mathbb{R}^n : \quad \alpha_i \in \left[1, \bar{z}_i^N\right], \quad i = 0, \dots, n-1, \quad \sum_{i=0}^{n-1} \alpha_i = N \right\} \tag{12}$$

with $\bar{z}_i^N := \min \left\{ \frac{N\left(\bar{x}_{i+1}^N - \bar{x}_i^N\right)}{L}, \frac{N\left(\bar{y}_{i+1}^N - \bar{y}_i^N\right)}{L} \right\}, \quad i = 0, \dots, n-1$

- **Approximate density reconstruction**[6] $\Rightarrow$ find optimal interaction parameter $\alpha$

$$\begin{aligned} & \underset{\alpha}{\text{minimize}} \quad \frac{1}{2} \left\| x(T) - \bar{y} \right\|^2 \\ \text{s.t.} \quad & \dot{x}(t) = V\left(W_\alpha x(t) + b_\alpha(t)\right) \\ & x(0) = \bar{x} \\ & \alpha \in \mathcal{A}_N \end{aligned} \tag{13}$$

- Existence of solutions guaranteed by assumptions on $V := v \circ \frac{1}{\cdot}$ (continuity of $v$) and constraints on $\alpha$ (compactness of $\mathcal{A}_N$)

[6] Baloul, Hayat, Liard, and Lissy 2025.

# ODE-Contrained Optimization

- Physical conditions on $\alpha := \alpha^N$ induce feasible set

$$\mathcal{A}_N := \left\{ \alpha \in \mathbb{R}^n : \quad \alpha_i \in \left[1, \bar{z}_i^N\right], \quad i = 0, \dots, n-1, \quad \sum_{i=0}^{n-1} \alpha_i = N \right\} \tag{12}$$

with $\bar{z}_i^N := \min \left\{ \frac{N\left(\bar{x}_{i+1}^N - \bar{x}_i^N\right)}{L}, \frac{N\left(\bar{y}_{i+1}^N - \bar{y}_i^N\right)}{L} \right\}, \quad i = 0, \dots, n-1$

- **Approximate density reconstruction**[6] $\Rightarrow$ find optimal interaction parameter $\alpha$

$$\begin{aligned} &\underset{\alpha}{\text{minimize}} \quad \frac{1}{2} \left\| x(T) - \bar{y} \right\|^2 \\ \text{s.t.} \quad &\dot{x}(t) = V\left(W_\alpha x(t) + b_\alpha(t)\right) \\ &x(0) = \bar{x} \\ &\alpha \in \mathcal{A}_N \end{aligned} \tag{13}$$

- Existence of solutions guaranteed by assumptions on $V := v \circ \frac{1}{\cdot}$ (continuity of $v$) and constraints on $\alpha$ (compactness of $\mathcal{A}_N$)
- No uniqueness (a priori) since nonlinear dynamics can lead to multiple minima

[6] Baloul, Hayat, Liard, and Lissy 2025.

# Learning Method

- Dataset consists of **artificial data** based on simulated (classical) FtL dynamics (3)
- Sampling of PVs yielding a **balanced representation** of overall traffic

- Dataset consists of **artificial data** based on simulated (classical) FtL dynamics (3)
- Sampling of PVs yielding a **balanced representation** of overall traffic
- Neural network architecture designed to **understand dynamics of traffic**

# Learning Method

- Dataset consists of **artificial data** based on simulated (classical) FtL dynamics (3)
- Sampling of PVs yielding a **balanced representation** of overall traffic
- Neural network architecture designed to **understand dynamics of traffic**
- Residual network (ResNet) where each block corresponds to a single time step
- Input $\bar{x}$ and state $x(.)$ is propagated by mirroring Euler discretization

$$x(t + \Delta t) = x(t) + V(Wx(t) + b)\Delta t \tag{14}$$

- Weights and biases $W, b$ are functions of $\alpha$

$$\begin{cases} W_{i,i} & := -\frac{N}{\alpha_i L}, i = 0, \ldots, n-1, \\ W_{i,i+1} & := \frac{N}{\alpha_i L}, i = 1, \ldots, n-2, \\ W_{i,j} & := 0, \text{otherwise}, \end{cases} \tag{15}$$

$$b_i(t) =:= \delta_{i,n} \frac{N}{\alpha_{n-1} L} \left( v_{\max} t + \bar{x}_n^N \right), \quad t \in [0, T] \tag{16}$$

- Nonlinear dynamic map $V$ acts as physics grounded activation function
- Backpropagation to minimize predictions errors $\frac{1}{n} \sum_{j=0}^{n} |x_j^{\alpha}(T) - \bar{y}_j^N|^2$

# Neural Network for Constrained Optimization

**Learning Architecture**

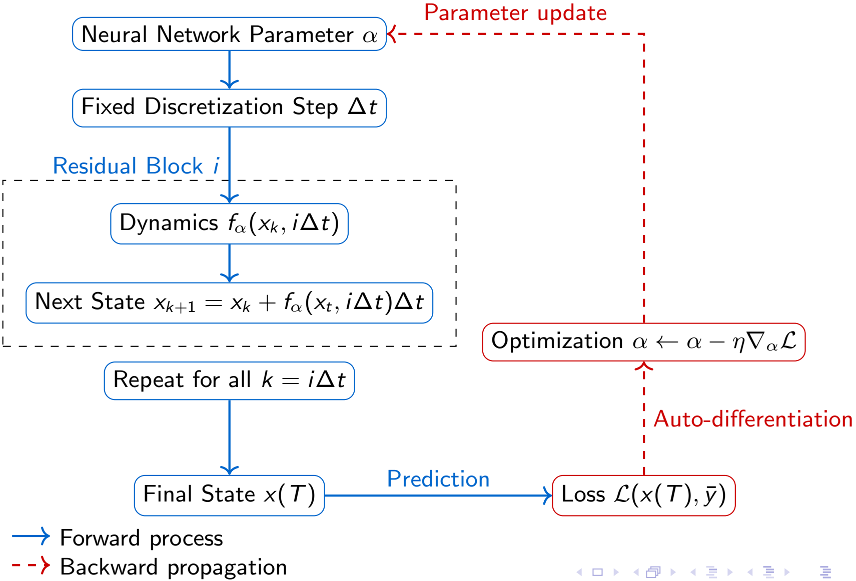

- Through optimal parameter $\bar{\alpha}$, training yields piecewise constant discrete density

$$\rho^N(t,x) = \sum_{i=0}^{n-1} \frac{\bar{\alpha}_i L}{N(x_{i+1}^N(t) - x_i^N(t))} \chi_{[x_i^N(t), x_{i+1}^N(t))}(x), \quad x \in \mathbb{R}, \quad t \in [0, T], \tag{17}$$

- Through optimal parameter $\bar{\alpha}$, training yields piecewise constant discrete density

$$\rho^N(t,x) = \sum_{i=0}^{n-1} \frac{\bar{\alpha}_i L}{N(x_{i+1}^N(t) - x_i^N(t))} \chi_{[x_i^N(t), x_{i+1}^N(t))}(x), \quad x \in \mathbb{R}, \quad t \in [0,T], \tag{17}$$

- Simulation on **test data** by solving ODE system

$$\begin{cases} \dot{x}_i^N(t) = v\left(\rho^N(t, x_i(t)^+)\right), & t \in (0,T], \\ x_i^N(0) = \bar{x}_i^N & i = 0, \dots, n_{\text{test}} \end{cases} \tag{18}$$

- Through optimal parameter $\bar{\alpha}$, training yields piecewise constant discrete density

$$\rho^N(t,x) = \sum_{i=0}^{n-1} \frac{\bar{\alpha}_i L}{N(x_{i+1}^N(t) - x_i^N(t))} \chi_{[x_i^N(t), x_{i+1}^N(t))}(x), \quad x \in \mathbb{R}, \quad t \in [0,T], \tag{17}$$

- Simulation on **test data** by solving ODE system

$$\begin{cases} \dot{x}_i^N(t) = v\left(\rho^N(t, x_i(t)^+)\right), & t \in (0,T], \\ x_i^N(0) = \bar{x}_i^N & i = 0, \dots, n_{\text{test}} \end{cases} \tag{18}$$

- Assess model's performance by measuring test error $\frac{1}{n_{\text{test}}} \sum_{j=0}^{n_{\text{test}}} |x_j(T) - \bar{y}_i^N|^2$

# Numerical experiments

- Parameters
  - Maximum traffic speed $v_{\max} = 120$ km/h
  - Maximum traffic density $\rho_{\max} = 200$ cars/km
  - Greenshields velocity $v(\rho) = v_{\max} \max\left\{1 - \frac{\rho}{\rho_{max}}, 0\right\}, \quad \rho \in [0, \rho_{max}]$
  - Final time horizon $T = 0.1$ h
- Sampling such 10% **of total fleet serve as PVs for training and** 2.5% **for testing**

- Parameters
  - Maximum traffic speed $v_{\max} = 120$ km/h
  - Maximum traffic density $\rho_{\max} = 200$ cars/km
  - Greenshields velocity $v(\rho) = v_{\max} \max\left\{1 - \frac{\rho}{\rho_{max}}, 0\right\}, \quad \rho \in [0, \rho_{max}]$
  - Final time horizon $T = 0.1$ h
- Sampling such 10% **of total fleet serve as PVs for training and** 2.5% **for testing**
- Three traffic scenarii modelled
  1. Shock wave represents an abrupt transition in traffic conditions
  2. Rarefaction wave represents a smooth transition in traffic condition
  3. Stop-and-go wave characterized by alternating regions of congestion and free flow

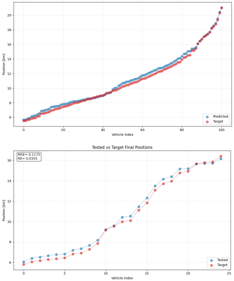


(a) $N = 1000$

Comparison of predicted and target final PV positions
**Top** Results from **training** procedure
**Bottom** Results on **test** sounds

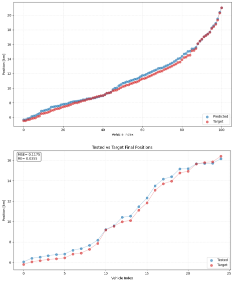


(a) $N = 1000$

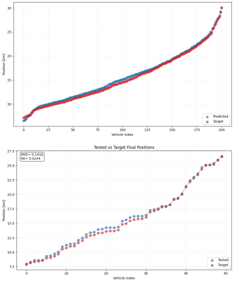


(b) $N = 2000$

Comparison of predicted and target final PV positions
**Top** Results from **training** procedure
**Bottom** Results on **test** sounds

# Shock wave scenario

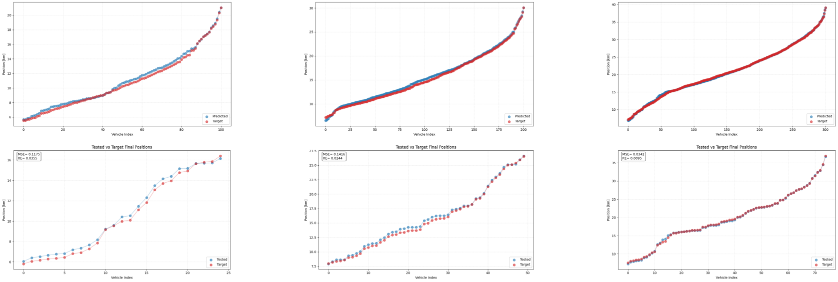


(a) $N = 1000$ (b) $N = 2000$ (c) $N = 3000$

Comparison of predicted and target final PV positions
**Top** Results from **training** procedure
**Bottom** Results on **test** sounds

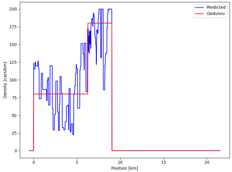


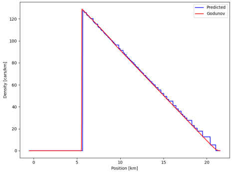


(a) $N = 1000$

Comparison of reconstructed and macroscopic densities
**Top** Initial densities
**Bottom** Final densities

# Shock wave scenario

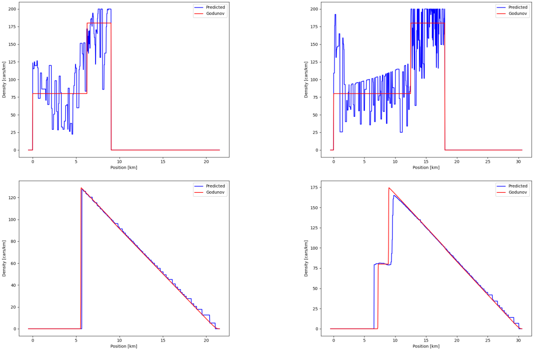


(a) $N = 1000$ (b) $N = 2000$

Comparison of reconstructed and macroscopic densities
**Top** Initial densities
**Bottom** Final densities

# Shock wave scenario

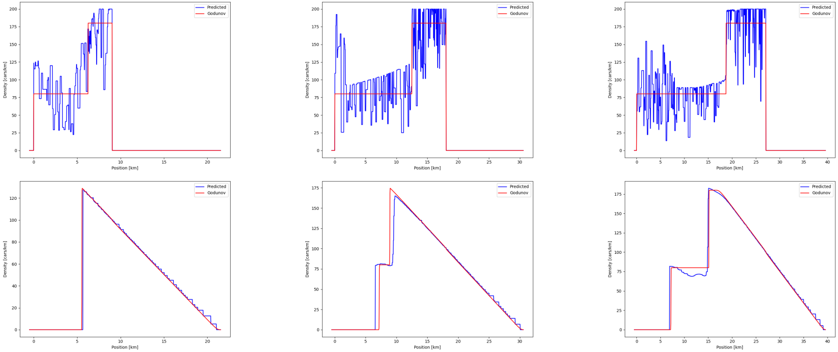


(a) $N = 1000$ (b) $N = 2000$ (c) $N = 3000$

Comparison of reconstructed and macroscopic densities
**Top** Initial densities
**Bottom** Final densities

# Shock wave scenario

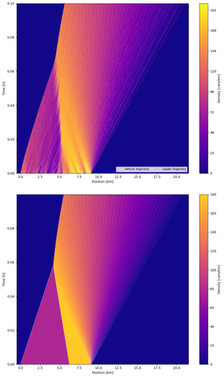


(a) $N = 1000$

Comparison of **reconstructed** and **macroscopic** densities
**Top** Reconstructed density from learning-based optimization
**Bottom** Macroscopic density from LWR PDE (Godunov scheme)

# Shock wave scenario

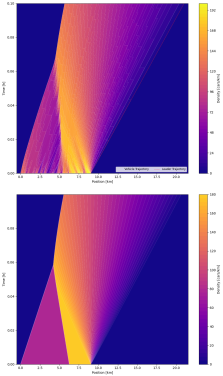


(a) $N = 1000$

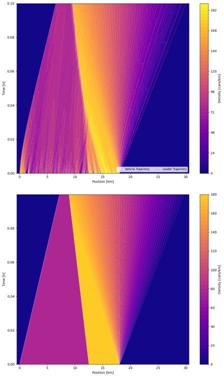


(b) $N = 2000$

Comparison of **reconstructed** and **macroscopic** densities
**Top** Reconstructed density from learning-based optimization
**Bottom** Macroscopic density from LWR PDE (Godunov scheme)

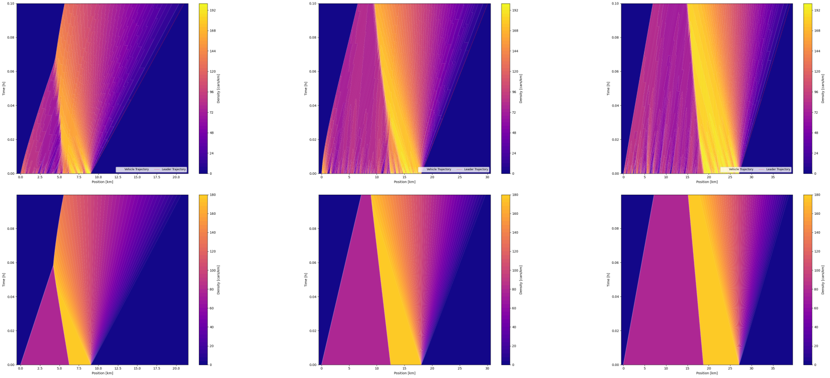

(a) $N = 1000$ (b) $N = 2000$ (c) $N = 3000$

Comparison of **reconstructed** and **macroscopic** densities
**Top** Reconstructed density from learning-based optimization
**Bottom** Macroscopic density from LWR PDE (Godunov scheme)

# Rarefaction wave scenario

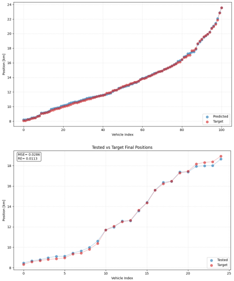


(a) $N = 1000$

Comparison of predicted and target final PV positions
**Top** Results from **training** procedure
**Bottom** Results on **test** sounds

# Rarefaction wave scenario

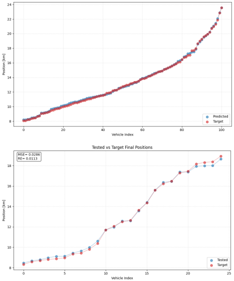

(a) $N = 1000$

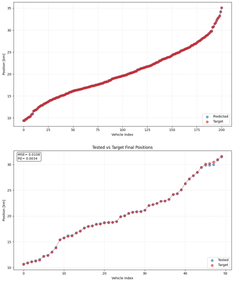

(b) $N = 2000$

Comparison of predicted and target final PV positions
**Top** Results from **training** procedure
**Bottom** Results on **test** sounds

# Rarefaction wave scenario

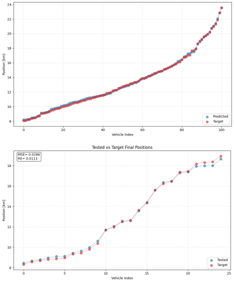


(a) $N = 1000$

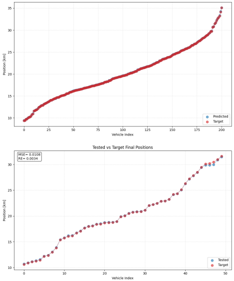


(b) $N = 2000$

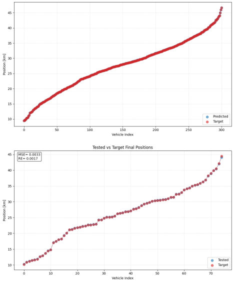


(c) $N = 3000$

Comparison of predicted and target final PV positions
**Top** Results from **training** procedure
**Bottom** Results on **test** sounds

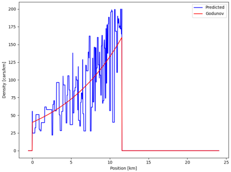


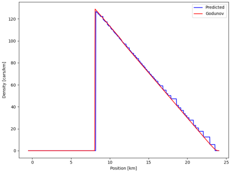


(a) $N = 1000$

Comparison of reconstructed and macroscopic densities
**Top** Initial densities
**Bottom** Final densities

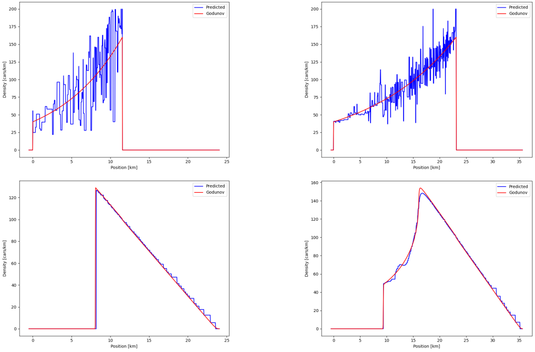


(a) $N = 1000$ (b) $N = 2000$

Comparison of reconstructed and macroscopic densities
**Top** Initial densities
**Bottom** Final densities

# Rarefaction wave scenario

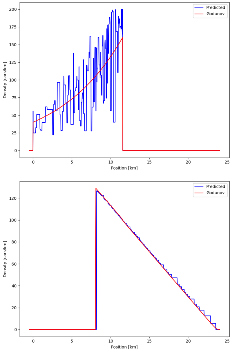


(a) $N = 1000$

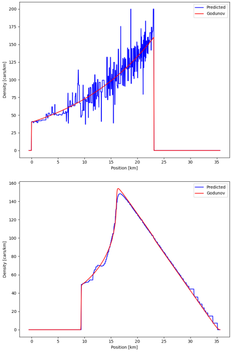


(b) $N = 2000$

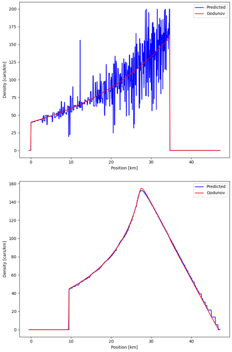


(c) $N = 3000$

Comparison of reconstructed and macroscopic densities
**Top** Initial densities
**Bottom** Final densities

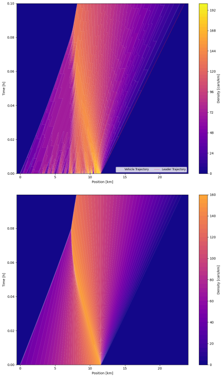


(a) $N = 1000$

Comparison of **reconstructed** and **macroscopic** densities
**Top** Reconstructed density from learning-based optimization
**Bottom** Macroscopic density from LWR PDE (Godunov scheme)

# Rarefaction wave scenario

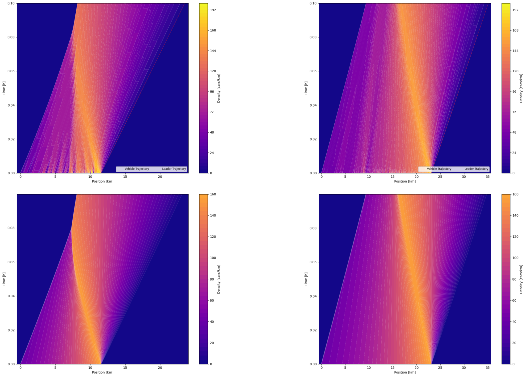

(a) $N = 1000$ (b) $N = 2000$

Comparison of **reconstructed** and **macroscopic** densities
**Top** Reconstructed density from learning-based optimization
**Bottom** Macroscopic density from LWR PDE (Godunov scheme)

# Rarefaction wave scenario

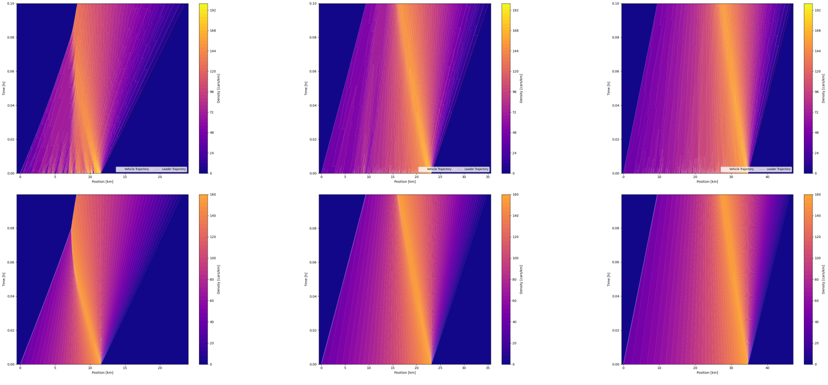


(a) $N = 1000$ (b) $N = 2000$ (c) $N = 3000$

Comparison of **reconstructed** and **macroscopic** densities
**Top** Reconstructed density from learning-based optimization
**Bottom** Macroscopic density from LWR PDE (Godunov scheme)

# Stop-and-go wave scenario

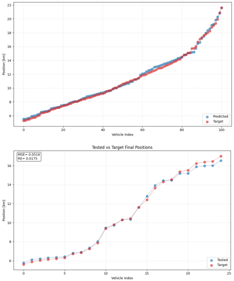


(a) $N = 1000$

Comparison of predicted and target final PV positions
**Top** Results from **training** procedure
**Bottom** Results on **test** sounds

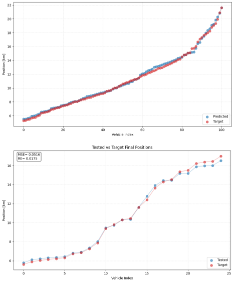


(a) $N = 1000$

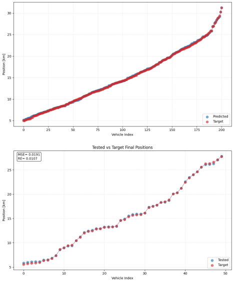


(b) $N = 2000$

Comparison of predicted and target final PV positions
**Top** Results from **training** procedure
**Bottom** Results on **test** sounds

# Stop-and-go wave scenario

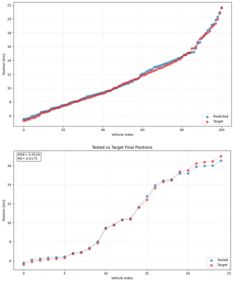


(a) $N = 1000$

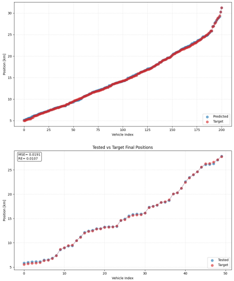


(b) $N = 2000$

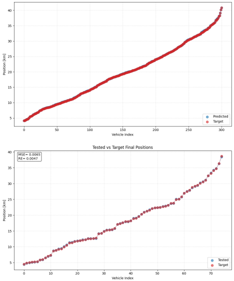


(c) $N = 3000$

Comparison of predicted and target final PV positions
**Top** Results from **training** procedure
**Bottom** Results on **test** sounds

# Stop-and-go wave scenario

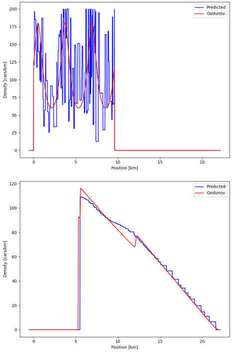


(a) $N = 1000$

Comparison of reconstructed and macroscopic densities
**Top** Initial densities
**Bottom** Final densities

# Stop-and-go wave scenario

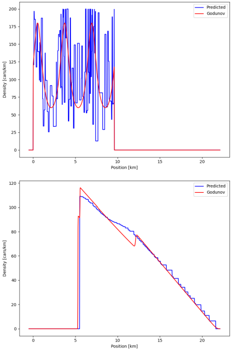


(a) $N = 1000$

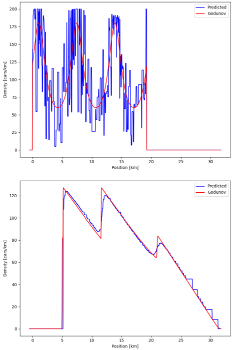


(b) $N = 2000$

Comparison of reconstructed and macroscopic densities
**Top** Initial densities
**Bottom** Final densities

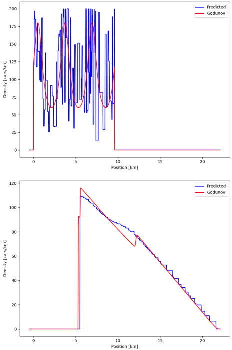


(a) $N = 1000$

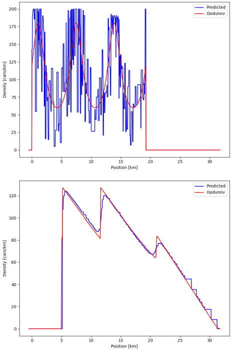


(b) $N = 2000$

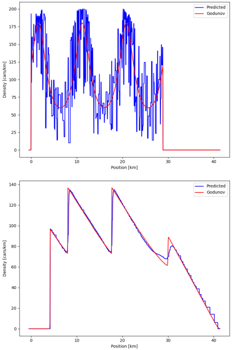


(c) $N = 3000$

Comparison of reconstructed and macroscopic densities
**Top** Initial densities
**Bottom** Final densities

# Stop-and-go wave scenario

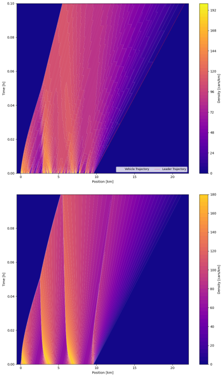


(a) $N = 1000$

Comparison of **reconstructed** and **macroscopic** densities
**Top** Reconstructed density from learning-based optimization
**Bottom** Macroscopic density from LWR PDE (Godunov scheme)

# Stop-and-go wave scenario

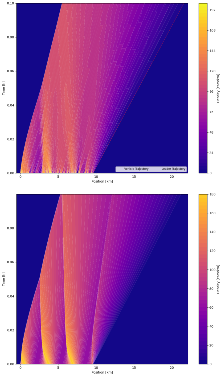

(a) $N = 1000$

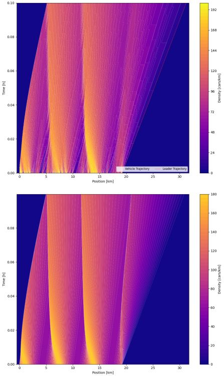

(b) $N = 2000$

Comparison of **reconstructed** and **macroscopic** densities
**Top** Reconstructed density from learning-based optimization
**Bottom** Macroscopic density from LWR PDE (Godunov scheme)

# Stop-and-go wave scenario

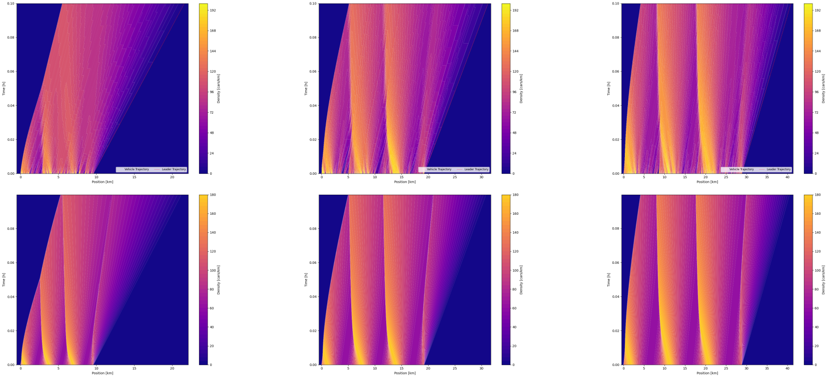


(a) $N = 1000$ (b) $N = 2000$ (c) $N = 3000$

Comparison of **reconstructed** and **macroscopic** densities
**Top** Reconstructed density from learning-based optimization
**Bottom** Macroscopic density from LWR PDE (Godunov scheme)

# Table of Contents

**Traffic State Reconstruction Approaches**

- Model-Based Method
  $\Rightarrow$ uses microscopic and macroscopic models
  $\Rightarrow$ provides theoretical guarantees
  $\Rightarrow$ struggles to capture real-world complexities
- Data-Driven Method
  $\Rightarrow$ learns patterns directly from measurement data
  $\Rightarrow$ derives system properties or predicts near-future states
  $\Rightarrow$ requires extensive data for effectiveness
- Our Approach
  $\Rightarrow$ combines models and data to address sparsity and improve realism
  $\Rightarrow$ **Integrates physical priors with data observations**
  $\Rightarrow$ achieves reliable traffic reconstruction with limited observations

- Conservation law with unilateral constraint[7] (toll gate)

$$\begin{cases} \text{LWR PDE (4) with} \\ f(\rho(t,0)) \leq q(t), & t > 0. \end{cases} \tag{19}$$

- Conservation law with moving bottleneck[8] (slow vehicle)

$$\begin{cases} \text{LWR PDE (4) with} \\ f\left(\rho(t,y(t))\right) - \dot{y}(t)\rho(t,y(t)) \leq \frac{\alpha\rho_{\max}}{4v_{\max}}\left(v_{\max} - \dot{y}(t)\right)^2, & t > 0, \\ \dot{y}(t) = \omega\left(\rho(t,y(t)_+)\right), & t > 0, \\ y(0) = y_0 \end{cases} \tag{20}$$

- Network with a junction[9] $J$ and $N$ incoming roads and $M$ outgoing ones

$$\begin{cases} \partial_t \rho_l(t,x) + \partial_x\left(f(\rho_l(t,x))\right) = 0, & t > 0, \quad x \in I_l, \quad l = 1,\dots,N+M \\ \rho_l(0,x) = \rho_{0,l}(x), & x \in I_l = [a_l, b_l], \quad l = 1,\dots,N+M \end{cases} \tag{21}$$

$\Rightarrow \sum_{i=1}^{N} f\left(\rho_i(t,(b_i)_-)\right) = \sum_{j=N+1}^{N+M} f\left(\rho_j(t,(a_j)_+)\right)$ (Rankine Hugoniot)

$\Rightarrow \sum_{i=1}^{N} f\left(\rho_i(t,(b_i)_-)\right)$ is maximized with $f\left(\rho_j(\cdot,(a_j)_+)\right) = \sum_{i=1}^{N} a_{j,i} f\left(\rho_i(\cdot,(b_i)_-)\right)$

[7] Colombo and Goatin 2007.

[8] Liard and Piccoli 2021.

[9] Coclite, Piccoli, and Garavello 2005.

## References I


Baloul, N., A. Hayat, T. Liard, and P. Lissy (2025). "Traffic Flow Reconstruction from Limited Collected Data". In: *hal preprint hal-05042012v1.*

Barreau, M., M. Aguiar, J. Liu, and K. H. Johansson (2021). "Physics-Informed Learning for Identification and State Reconstruction of Traffic Density". In: *arXiv preprint arXiv:2103.13852.*

Coclite, G. M., B. Piccoli, and G. Garavello (2005). "Traffic Flow on a Road Network". In: *SIAM Journal on Mathematical Analysis* 36.6, pp. 1862–1886.

Colombo, R. M. and P. Goatin (2007). "A Well-Posed Conservation Law with a Variable Unilateral Constraint". In: *Journal of Differential Equations* 234.2, pp. 654–675.

Di Francesco, M., S. Fagioli, M. D. Rosini, and G. Russo (2016). "Follow-the-Leader Approximations of Macroscopic Models for Vehicular and Pedestrian Flows". In: *arXiv preprint arXiv:1610.06743.*

Di Francesco, M. and M. D. Rosini (2015). "Rigorous Derivation of Nonlinear Scalar Conservation Laws from Follow-the-Leader Type Models via Many Particle Limit". In: *arXiv preprint arXiv:1404.7062.*

Holden, H. and N. H. Risebro (2017). "The Continuum Limit of Follow-the-Leader Models: A Short Proof". In: *arXiv preprint arXiv:1709.07661.*

Liard, T. and B. Piccoli (2021). "On entropic solutions to conservation laws coupled with moving bottlenecks". In: *Communications in Mathematical Sciences* 19.4, pp. 1041–1068.

Liu, J., M. Barreau, M. Cicic, and K. H. Johansson (2020). "Learning-Based Traffic State Reconstruction Using Probe Vehicles". In: *arXiv preprint arXiv:2011.05031*.

# Scheme of Model

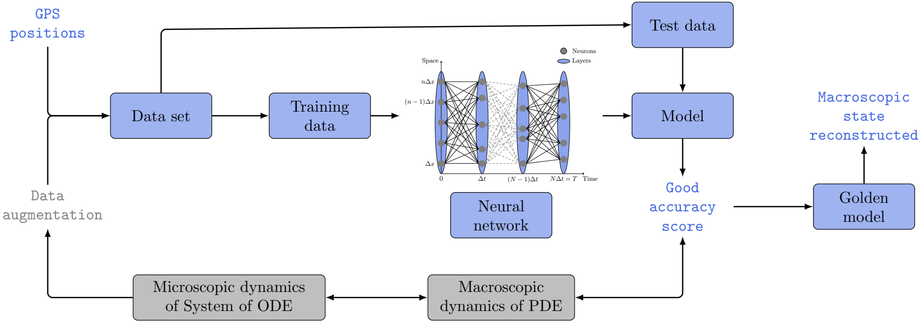


Traffic Flow Reconstruction Pipeline

- Weak solution of (4) is entropy admissible if it satisfies Kruzhkov entropy condition

$$\int_0^T \int_{\mathbb{R}} |u-k| \frac{\partial \phi}{\partial t} + \mathrm{sign}(u-k)(f(u)-f(k)) \frac{\partial \phi}{\partial x} dxdt \geq 0, \quad \forall k \in \mathbb{R} \tag{22}$$

**Convergence of approximate density to solution of LWR**

Under some assumptions, piecewise-constant density

$$\rho^N(t,x) = \sum_{i=0}^{n-1} \frac{\bar{\alpha}_i^N L}{N(x_{i+1}^N(t) - x_i^N(t))} \chi_{[x_i^N(t), x_{i+1}^N(t))}(x), \quad x \in \mathbb{R}, \quad t \in [0,T], \tag{23}$$

where $\bar{\alpha}_i^N \in \mathcal{A}_N$ is a solution to (13) converges to **unique entropy** solution $\rho$ of

$$\begin{aligned} &\frac{\partial \rho}{\partial t}(t,x) + \frac{\partial f(\rho)}{\partial x}(t,x) = 0, \quad x \in \mathbb{R}, \quad t \in [0,T], \\ &\rho(0,x) = \rho_0(x), \quad x \in \mathbb{R}. \end{aligned} \tag{24}$$

- Typically, we impose a condition of type

$$\max_{i=0,\dots,n-1} \alpha_i^N = o(N). \tag{25}$$

$\Rightarrow$ ensures controlled growth of $\alpha_N$